

Supporting Information

**Metal-free Polymeric and Molecular Disorder/Order Semiconductor
Heterojunction for Visible-light Photocatalytic Minisci-Type
Reaction**

*Peihe Li,^a * Qingguang Li,^a Gelan Wang,^a Ye Lu,^a Limei Duan^a Jie Bai,^c Sarina Sarina,^b and Jinghai Liu^a, **

^aInner Mongolia Key Laboratory of Carbon Nanomaterials, College of Chemistry and Materials Science, Inner Mongolia Minzu University, Tongliao, 028000, China. *E-mail:* phli2018@foxmail.com; jhliu2008@sinano.ac.cn.

^bSchool of Chemical and Biomolecular Engineering, Faculty of Engineering, The University of Sydney, Camperdown, NSW 2037, Australia.

^cChemical Engineering College, Inner Mongolia University of Technology, Huhhot, 010051, China

Supporting Information Table of Contents

1	Figure S1. UV-Vis DRS spectrum of PTCDA, g-C ₃ N ₄ , and PTCDA/g-C ₃ N ₄ .	S3
2	Figure S2. Tauc plot of the UV-Vis DRS spectrum of PTCDA, g-C ₃ N ₄ and PTCDA/g-C ₃ N ₄ .	S4
3	Figure S3. IR spectra of the PTCDA, g-C ₃ N ₄ , and PTCDA/ g-C ₃ N ₄ .	S5
4	Figure S4. Specific surface area (SSA) and BJH pore size distributions for g-C ₃ N ₄ and PTCDA/g-C ₃ N ₄ .	S6
5	Figure S5. XPS spectra of PTCDA, g-C ₃ N ₄ , and PTCDA/g-C ₃ N ₄ .	S7
6	Figure S6. VB-XPS of PTCDA and g-C ₃ N ₄ .	S8
7	Figure S7. The emission spectrum of experiment lamps.	S9
8	Figure S8. UV-Vis absorption spectra of the permanganate disappear.	S10
9	Figure S9. The open-loop of 2a under the UV and 365 nm LED light irradiation.	S11
10	Scheme S1. Radical-trapping experiments and Kinetic isotope effect (KIE) experiment.	S12
11	Quantum efficiency calculations.	S13
12	Figure S10. Electrochemical impedance spectra of g-C ₃ N ₄ and PTCDA/g-C ₃ N ₄ .	S14
13	Figure S11. Tapping-mode AFM images in air for the electrode surface. (a) g-C ₃ N ₄ , (b) PTCDA, (c) PTCDA/g-C ₃ N ₄ .	S15
14	Figure S12. The molecular structure of PTCDA and PTCDI.	S15
15	Figure S13. Reusability tests using the isolated PTCDA/g-C ₃ N ₄ photocatalyst	S16
16	Spectroscopic data of products	S17
17	NMR Spectra	S22
18	HRMS of 3i	S31

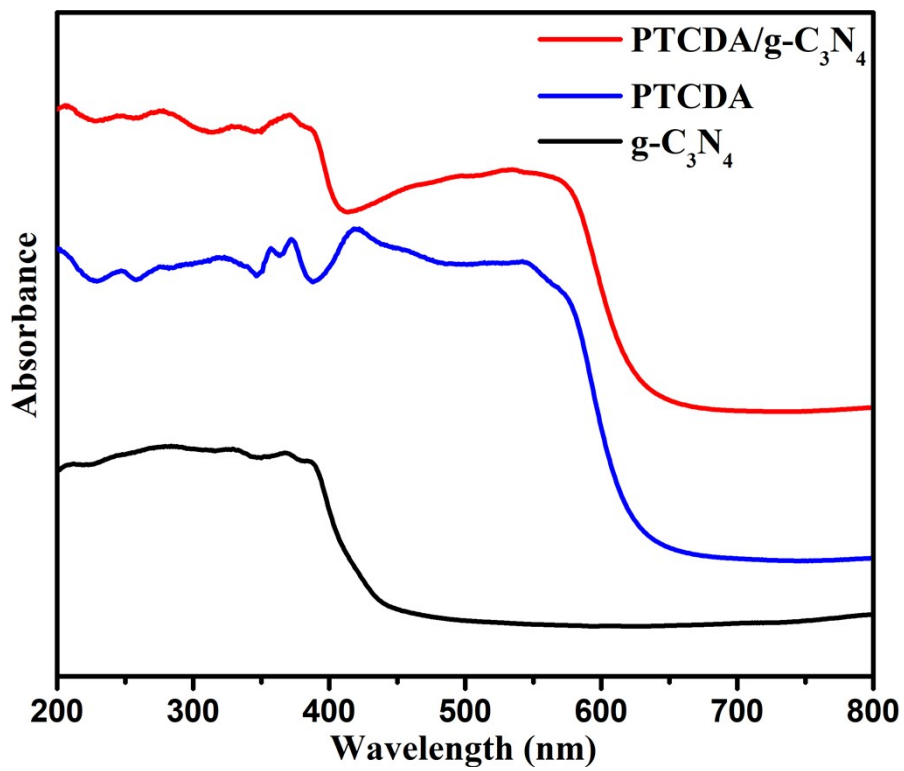


Figure S1. UV-Vis DRS spectrum of PTCDA, g-C₃N₄, and PTCDA/g-C₃N₄.

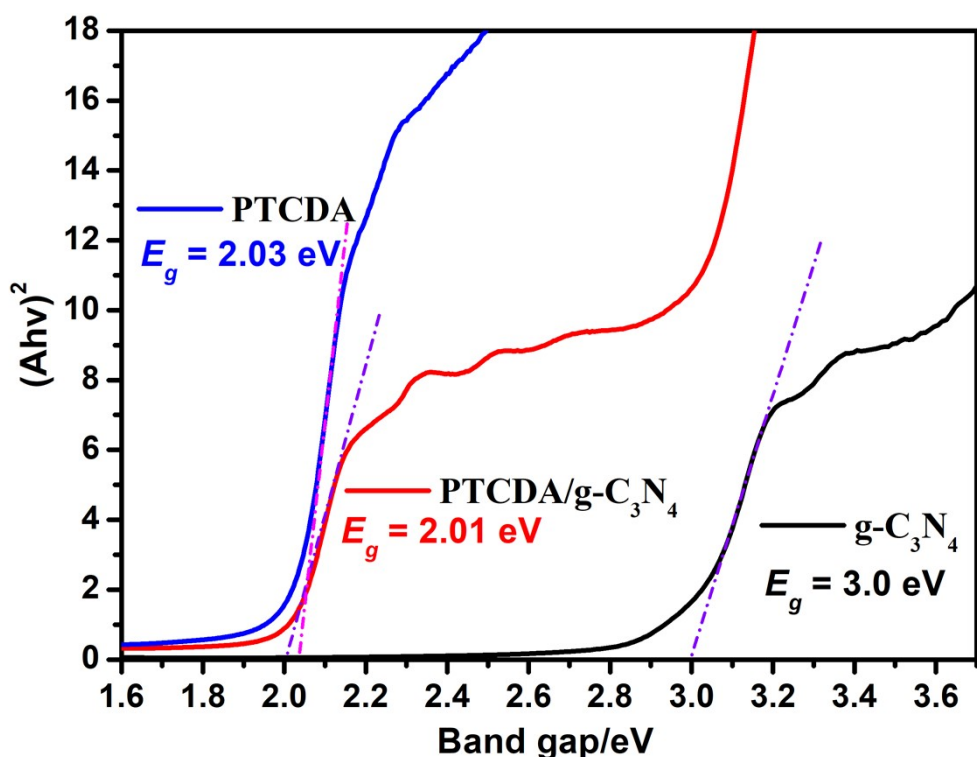


Figure S2. Tauc plot of the UV-Vis DRS spectrum of PTCDA, g-C₃N₄ and PTCDA/g-C₃N₄.

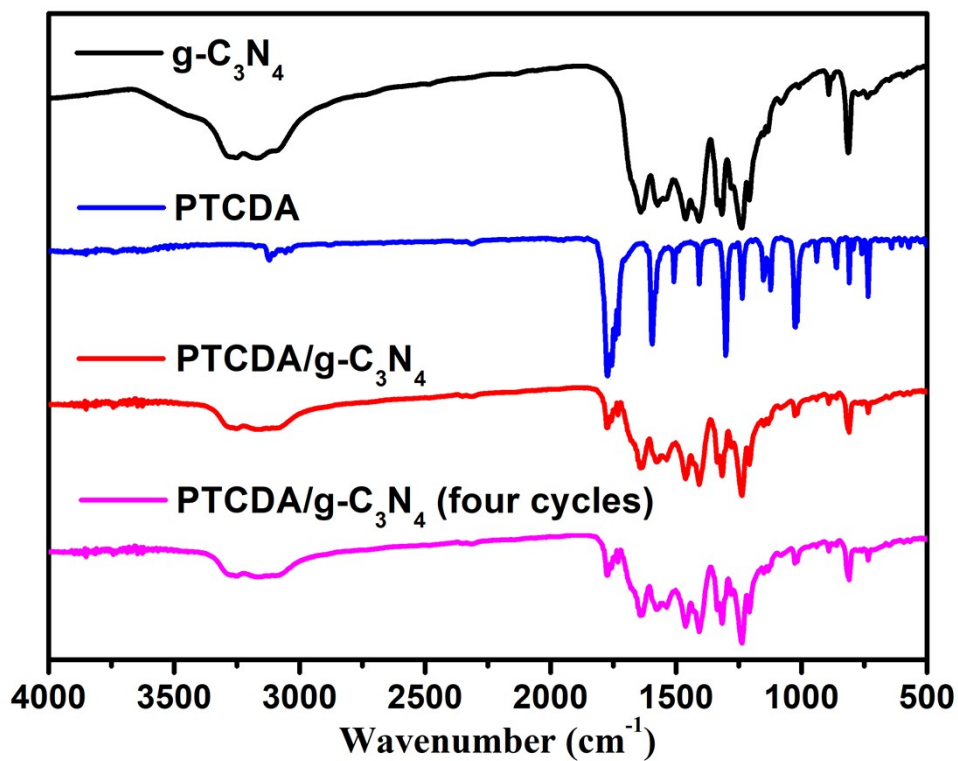


Figure S3. IR spectra of the $\text{g-C}_3\text{N}_4$ (black), PTCDA (blue), and as-prepared PTCDA/ $\text{g-C}_3\text{N}_4$ (red).

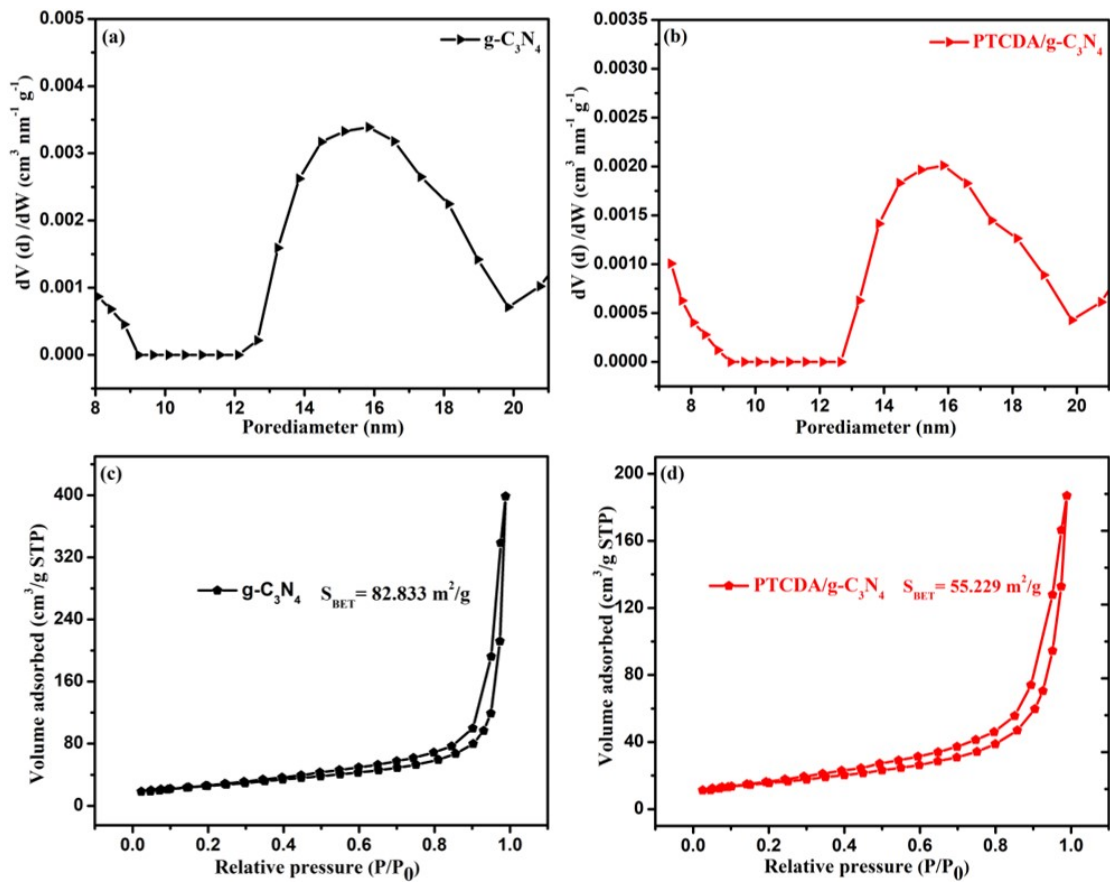


Figure S4. Specific surface area (SSA) and BJH pore size distributions for $\text{g-C}_3\text{N}_4$ and $\text{PTCDA/g-C}_3\text{N}_4$. (a) and (b) pore size distribution and pore volume analyzed according to Barret-Joyner-Halenda (BJH) method for $\text{g-C}_3\text{N}_4$ and $\text{PTCDA/g-C}_3\text{N}_4$. N₂ adsorption/desorption isotherms: (c) the SSA of $\text{g-C}_3\text{N}_4$ is $82.833 \text{ m}^2/\text{g}$, and (d) $\text{PTCDA/g-C}_3\text{N}_4$ is $55.229 \text{ m}^2/\text{g}$.

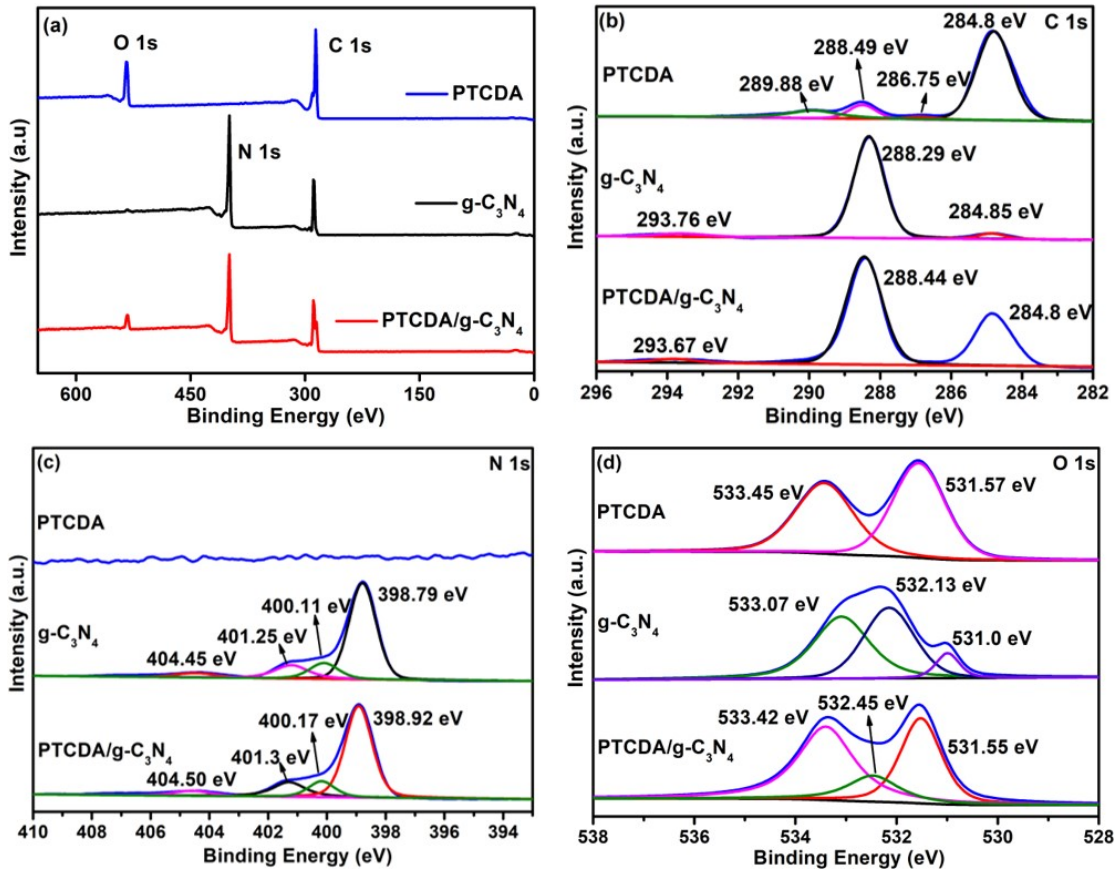


Figure S5. XPS spectra: (a) A whole scanning XPS spectra. (b) C 1s of the PTCDA, g-C₃N₄, and PTCDA/g-C₃N₄. (c) N 1s of the PTCDA, g-C₃N₄, and PTCDA/g-C₃N₄. (d) O 1s of the PTCDA, g-C₃N₄, and PTCDA/g-C₃N₄.

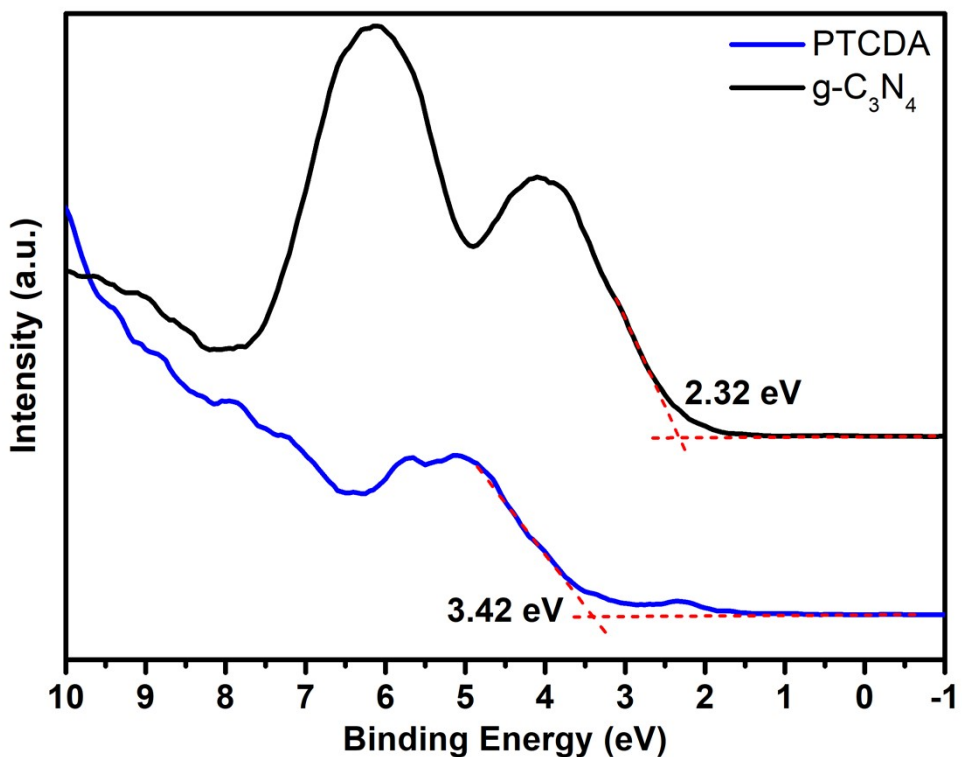


Figure S6. VB-XPS of PTCDA and $\text{g-C}_3\text{N}_4$.

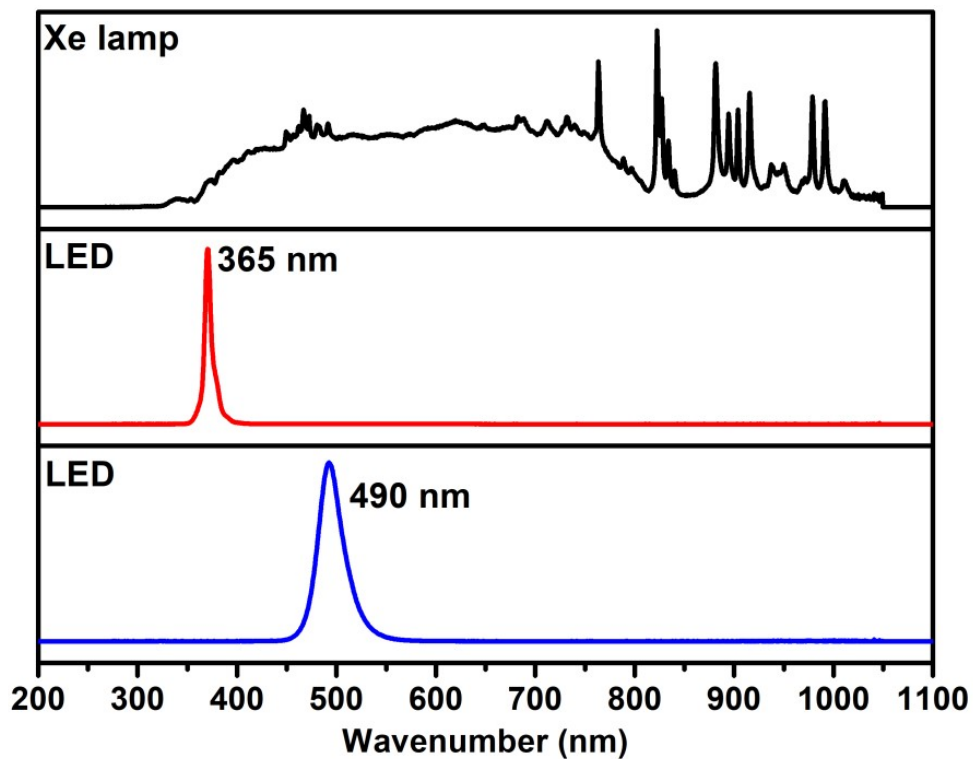


Figure S7. The emission spectrum of experiment lamps (Xe lamp and light-emitting diode (LED)).

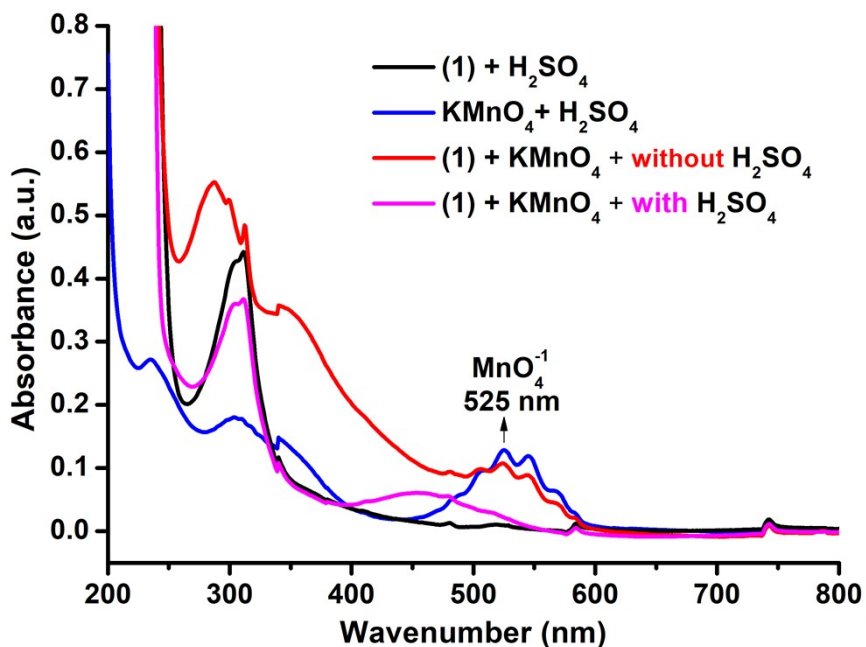
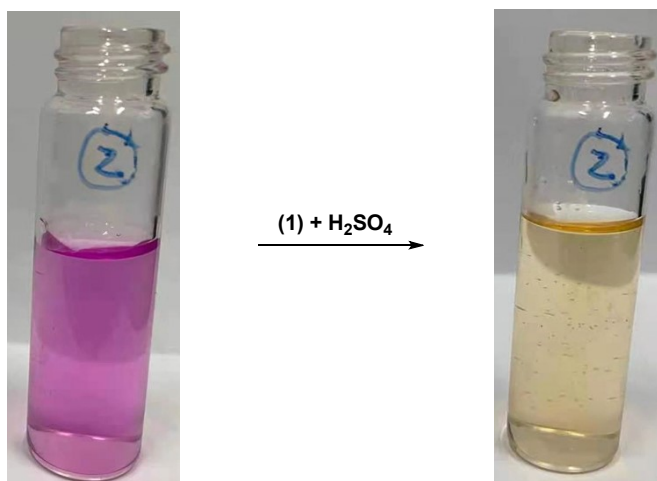
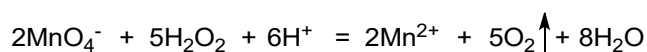


Figure S8. UV-Vis absorption spectra of the permanganate (MnO_4^{-1}) disappeared after addition the catalytic reaction solution ((1) = the reaction solution after photocatalysis).

We confirmed the formation of H₂O₂ by UV/Vis monitor of the disappear of the permanganate (MnO_4^{-1}) in aqueous solution. When the over amount of (1) (the reaction solution after photocatalysis) was added in the permanganate (MnO_4^{-1}) solution (5 mL, 0.2 mM) in the presence of hydrogen ions (H⁺) (1 mL, 2M H₂SO₄), the MnO_4^- can be reduced to Mn²⁺, which shows the disappear of the characteristic peaks at ca. 450-600 nm (maximum absorption peak at 525 ± 1 nm) in UV/Vis spectra. At the same time, the red color of potassium permanganate solution disappeared (See the following picture).



MnO₄⁻ solution 5 mL (0.2 mM)

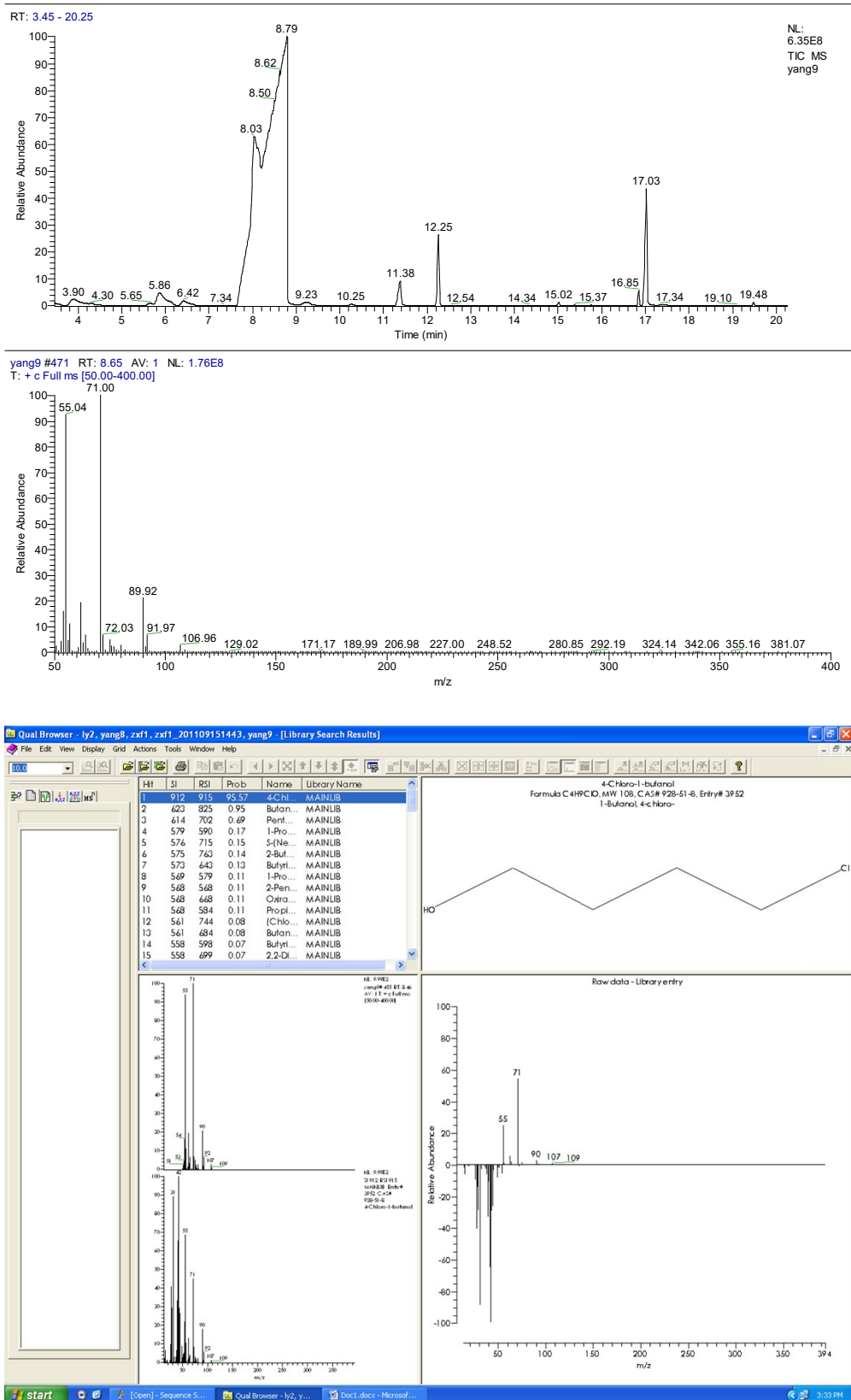


Figure S9. The open-loop of **2a** under the UV and 365 nm LED light irradiation.

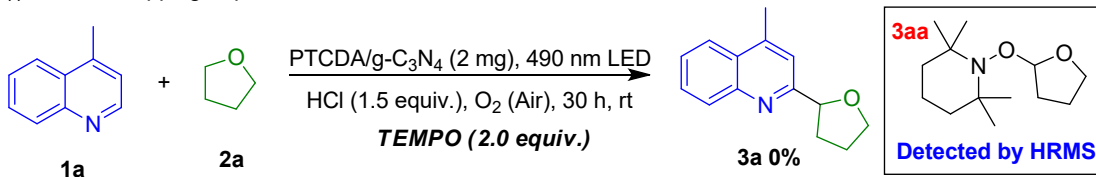
Radical-trapping experiments and Kinetic isotope effect (KIE) experiment.

Radical-trapping experiments (i): The reaction was performed in a 20 mL quartz vial with 2 mL tetrahydrofuran containing 2 mg PTCDA/g-C₃N₄ photocatalyst, 1.5 equiv of HCl (36-38 wt%), 0.5 mmol 4-methylquinoline and 2,2,6,6-Tetramethyl-1-piperidinyloxy (TEMPO) (2 equiv.) at room temperature under air conditions. The reactor was illuminated by a 490 nm LED light with a light intensity of 7.05 mW cm⁻² for 30 h (**Scheme S1**).

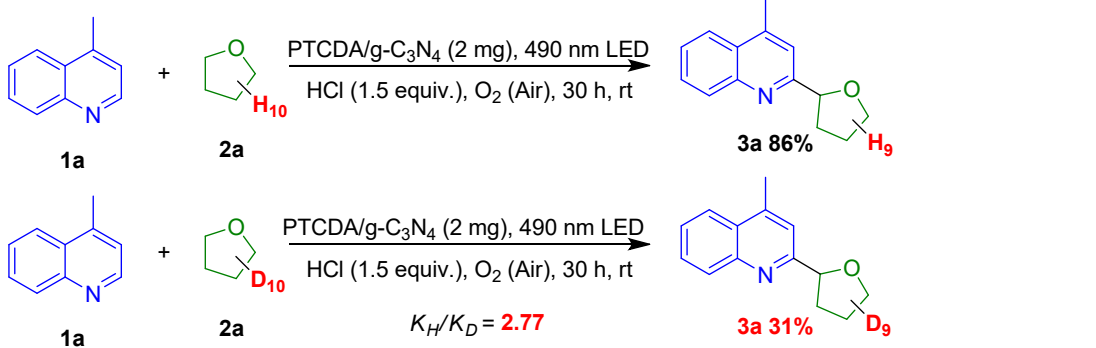
Kinetic isotope effect (KIE) experiment (ii): The reaction was performed in a 20 mL quartz vial with 2 mL tetrahydrofuran or tetrahydrofuran-D8 (CAS: 1693-74-9) containing 2 mg PTCDA/g-C₃N₄ photocatalyst, 1.5 equiv of HCl (36-38 wt%), 0.5 mmol 4-methylquinoline at room temperature under air conditions. The reactor was illuminated by a 490 nm LED light with a light intensity of 7.05 mW cm⁻² for 30 h (**Scheme S1**). After completion of the reaction, the catalyst was separated by centrifugation and washed with ethyl acetate. The reaction was quenched with 5 mL saturated ammonium chloride, 5 mL saturated sodium bicarbonate, and extracted with ethyl acetate (3×10 mL), the organic layer was washed with H₂O, brine, dried over MgSO₄, and purified by silica gel flash chromatography using a mixture of petroleum ether and ethyl acetate to provide the desired product.

Scheme S1. Mechanistic experiments.

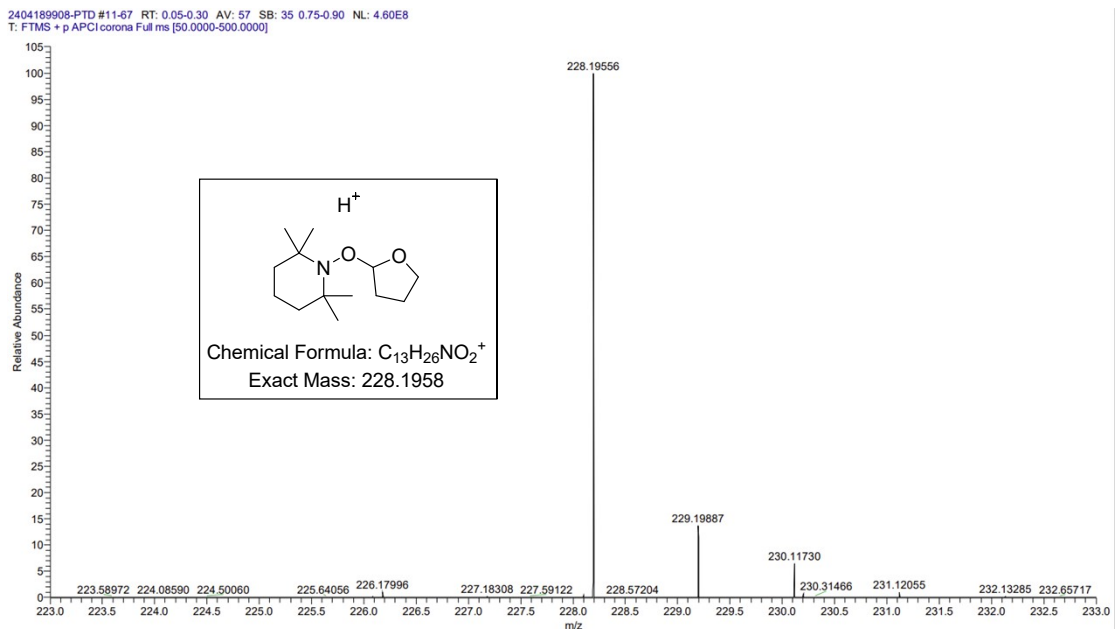
(i) Radical-Trapping Experiments



(ii) Kinetic Isotopic Effect Experiment



TEMPO trapped product **3aa** is confirmed by HRMS



Quantum efficiency calculations.

The QE determination at $\lambda_0 = 490$ nm. The catalyst solution was irradiated by a 15 W LED with a $\lambda_0 \pm 20$ nm band-pass filter for 30 hours. The average intensity of irradiation was determined to be 7.05 mW/cm^2 by an ILT 950 spectroradiometer (International Light Technologies) and the irradiation area was 3.02 cm^2 . The number of incident photons (N) is 5.668×10^{21} as calculated by equation (1). The yield of **3a** is 86%, The amount of **3a** molecules generated in 30 hours was $0.5 \times 86\%$ mmol. The quantum efficiency is calculated from equation (2).

$$N = \frac{E\lambda}{hc} = \frac{7.05 \times 10^{-3} \times 3.02 \times 30 \times 3600 \times 490 \times 10^{-9}}{6.626 \times 10^{-34} \times 3 \times 10^8} \left(\frac{\text{W/cm}^2 \times \text{cm}^2 \times \text{s} \times \text{m}}{\text{J} \cdot \text{s} \times \text{m/s}} \right) = 5.668 \times 10^{21} \quad (1)$$

$$\begin{aligned} QE &= \frac{2 \times \text{the number of evolved H}_2 \text{ molecules}}{\text{the number of incident photons}} \times 100\% \\ &= \frac{2 \times 6.02 \times 10^{23} \times 0.5 \times 0.86 \times 10^{-3}}{5.668 \times 10^{21}} \times 100\% = 9.13\% \quad (2) \end{aligned}$$

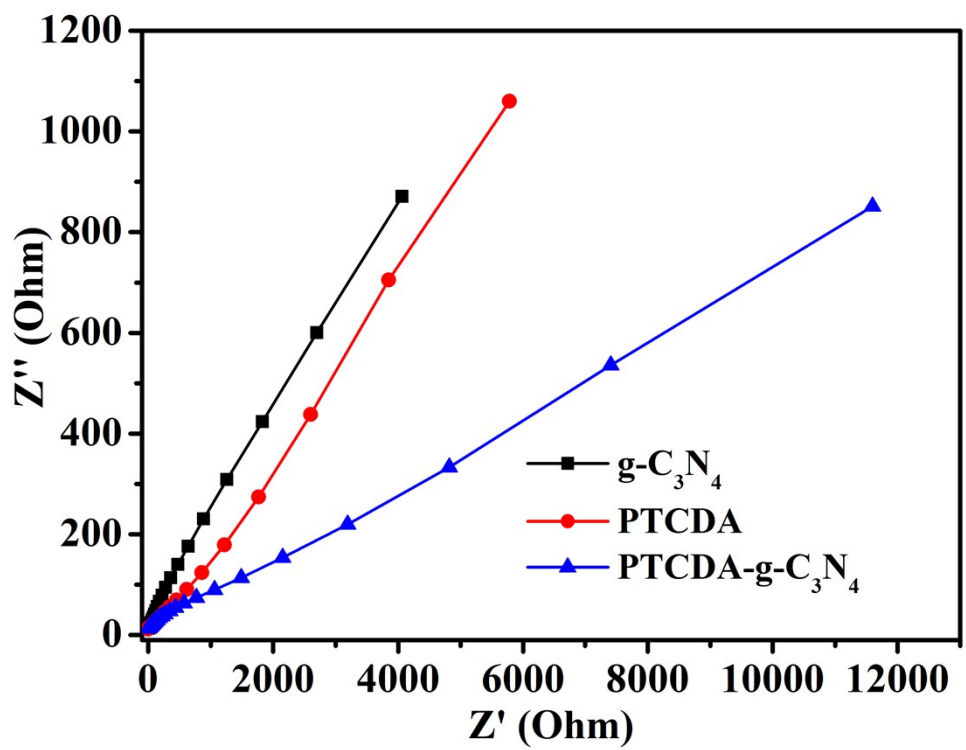


Figure S10. Electrochemical impedance spectroscopy (EIS) spectra of $\text{g-C}_3\text{N}_4$, PTCDA and PTCDA/g-C₃N₄.

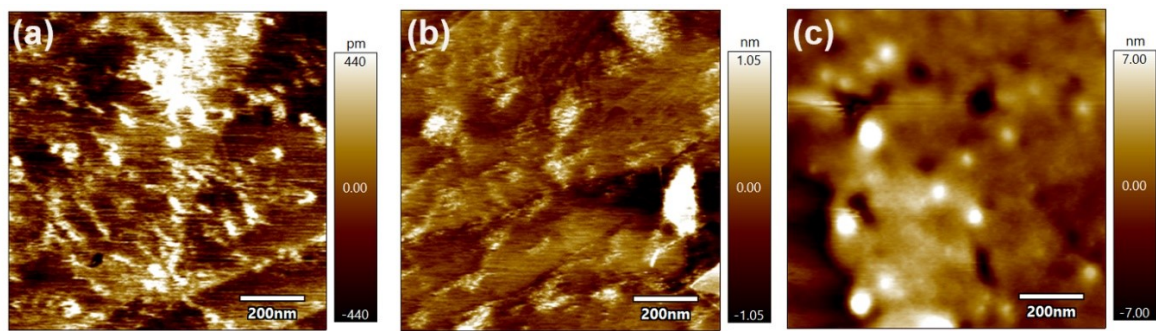


Figure S11. Tapping-mode AFM images in air for the electrode surface. (a) g-C₃N₄, (b) PTCDA, (c) PTCDA/g-C₃N₄.

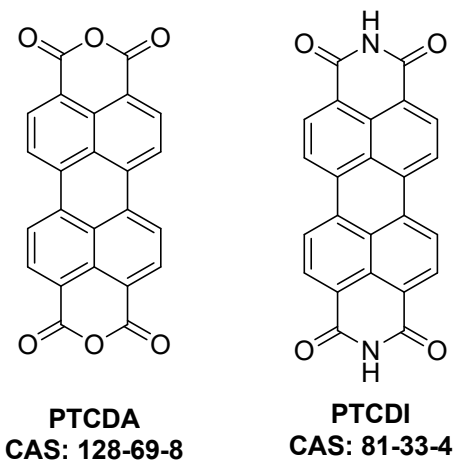


Figure S12. The molecular structure of PTCDA and PTCDI.

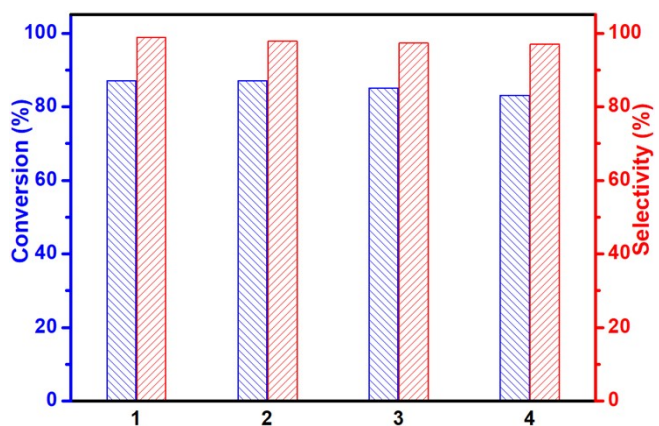
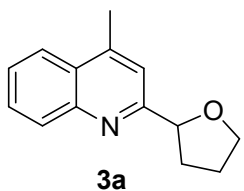


Figure S13. Reusability tests using the isolated PTCDA/g-C₃N₄ photocatalyst
(Legend: blue bar, **1a** conversion; red bar, **3a** selectivity.).

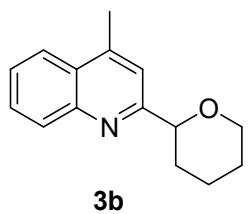
Spectroscopic data of products

Table 3, entry 1



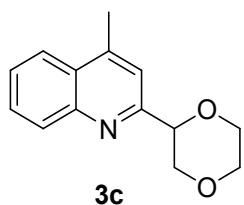
4-methyl-2-(tetrahydrofuran-2-yl)quinolone (3a). Oil; $R_f = 0.5$ (hexane:EtOAc = 20:1); ^1H NMR (500 MHz, CDCl_3) δ 8.05 (d, $J = 8.4$ Hz, 1H), 7.96 (d, $J = 8.3$ Hz, 1H), 7.68 (t, $J = 7.1$ Hz, 1H), 7.52 (t, $J = 7.1$ Hz, 1H), 7.44 (s, 1H), 5.13 (t, $J = 7.0$ Hz, 1H), 4.17 (dd, $J = 14.8, 6.7$ Hz, 1H), 4.03 (dd, $J = 14.8, 6.8$ Hz, 1H), 2.70 (s, 3H), 2.50 (dd, $J = 11.8, 5.5$ Hz, 1H), 2.23-1.81 (m, 3H); ^{13}C NMR (125 MHz, CDCl_3) δ 163.5, 147.7, 145.3, 129.9, 129.5, 127.8, 126.2, 124.0, 119.0, 82.4, 69.6, 33.7, 26.3, 19.3. (Spectra data are consistent with those reported in the literature: H. Zhao, Z. Li and J. Jin, *New J. Chem.*, **2019**, *43*, 12533-12537.)

Table 3, entry 2



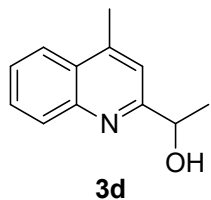
4-methyl-2-(tetrahydro-2H-pyran-2-yl)quinolone (3b). Oil; $R_f = 0.5$ (hexane:EtOAc = 20:1); ^1H NMR (500 MHz, CDCl_3) δ 8.06 (d, $J = 8.4$ Hz, 1H), 7.97 (d, $J = 8.3$ Hz, 1H), 7.68 (t, $J = 7.6$ Hz, 1H), 7.52 (t, $J = 7.6$ Hz, 1H), 7.46 (s, 1H), 4.60 (d, $J = 11.1$ Hz, 1H), 4.21 (d, $J = 11.2$ Hz, 1H), 3.69 (t, $J = 11.1$ Hz, 1H), 2.71 (s, 3H), 2.09 (d, $J = 13.0$ Hz, 1H), 1.98 (s, 1H), 1.76 (t, $J = 9.2$ Hz, 2H), 1.64 (t, $J = 11.2$ Hz, 2H); ^{13}C NMR (125 MHz, CDCl_3) δ 162.0, 147.0, 144.9, 129.5, 128.9, 127.4, 125.7, 123.5, 118.7, 81.5, 68.8, 32.7, 25.7, 23.6, 18.7. (Spectra data are consistent with those reported in the literature: H. Zhao, Z. Li and J. Jin, *New J. Chem.*, **2019**, *43*, 12533-12537.)

Table 3, entry 3



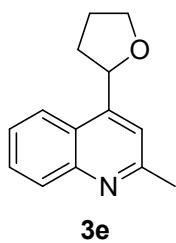
2-(1,4-dioxan-2-yl)-4-methylquinoline (3c). White solid; $R_f = 0.5$ (hexane:EtOAc = 20:1); ^1H NMR (500 MHz, CDCl_3) δ 8.07 (d, $J = 8.3$ Hz, 1H), 7.98 (d, $J = 8.3$ Hz, 1H), 7.70 (t, $J = 8.3$ Hz, 1H), 7.55 (t, $J = 7.0$ Hz, 1H), 7.46 (s, 1H), 4.90 (dd, $J = 10.1, 2.8$ Hz, 1H), 4.23 (dd, $J = 11.6, 2.7$ Hz, 1H), 4.01 (dd, $J = 10.4, 2.7$ Hz, 2H), 3.82 (dd, 2H), 3.63 (t, 1H), 2.72 (s, 3H); ^{13}C NMR (125 MHz, CDCl_3) δ 158.2, 147.6, 145.6, 130.1, 129.7, 128.0, 126.6, 124.1, 119.5, 79.2, 71.5, 67.5, 66.8, 19.3. (Spectra data are consistent with those reported in the literature: H. Zhao, Z. Li and J. Jin, *New J. Chem.*, **2019**, 43, 12533-12537.)

Table 3, entry 4



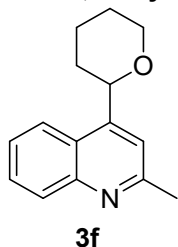
1-(4-methylquinolin-2-yl)ethanol (3d). Oil; $R_f = 0.6$ (hexane:EtOAc = 20:1); ^1H NMR (500 MHz, CDCl_3) δ 8.07 (d, $J = 8.4$ Hz, 1H), 7.99 (d, $J = 8.3$ Hz, 1H), 7.71 (t, $J = 7.6$ Hz, 1H), 7.56 (t, $J = 7.6$ Hz, 1H), 7.18 (s, 1H), 5.14 (br s, 1H), 4.99 (dd, $J = 6.6$ Hz, 1H), 2.72 (s, 3H), 1.57 (d, $J = 6.6$ Hz, 3H); ^{13}C NMR (125 MHz, CDCl_3) δ 162.4, 146.1, 145.3, 129.5, 129.3, 127.5, 126.2, 123.8, 118.6, 68.6, 24.1, 19.0. (Spectra data are consistent with those reported in the literature: H. Zhao, Z. Li and J. Jin, *New J. Chem.*, **2019**, 43, 12533-12537.)

Tabel 3, entry 5



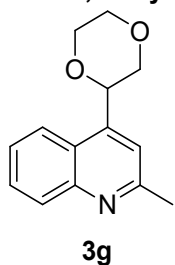
2-methyl-4-(tetrahydrofuran-2-yl)quinolone (3e). Oil; $R_f = 0.5$ (hexane:EtOAc = 20:1); ^1H NMR (500 MHz, CDCl_3) δ 8.06 (d, $J = 8.4$ Hz, 1H), 7.85 (d, $J = 8.3$ Hz, 1H), 7.67 (t, $J = 7.6$ Hz, 1H), 7.49 (t, $J = 7.2$ Hz, 1H), 7.45 (s, 1H), 5.58 (t, $J = 7.1$ Hz, 1H), 4.23 (td, $J = 7.6, 5.7$ Hz, 1H), 4.05 (dd, $J = 15.3, 7.2$ Hz, 1H), 2.74 (s, 3H), 2.65–2.58 (m, 1H), 2.21–1.97 (m, 2H), 1.88–1.81 (m, 1H); ^{13}C NMR (125 MHz, CDCl_3) δ 159.4, 148.1, 129.7, 129.6, 129.4, 125.9, 124.2, 123.4, 117.6, 75.7, 69.4, 34.3, 26.4, 25.8. (Spectra data are consistent with those reported in the literature: A. Vijeta and E. Reisner, *Chem. Commun.*, **2019**, 55, 14007–14010.)

Table 3, entry 6



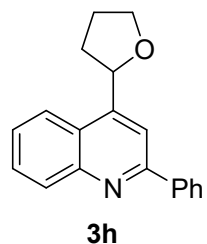
2-methyl-4-(tetrahydro-2H-pyran-2-yl)quinolone (3f). Oil; $R_f = 0.45$ (hexane:EtOAc = 20:1); ^1H NMR (500 MHz, CDCl_3) δ 8.05 (d, $J = 8.4$ Hz, 1H), 7.92 (d, $J = 8.4$ Hz, 1H), 7.65 (t, $J = 7.6$ Hz, 1H), 7.48 (t, $J = 7.7$ Hz, 1H), 7.45 (s, 1H), 5.02 (d, $J = 10.0$ Hz, 1H), 4.26 (d, $J = 10.0$ Hz, 1H), 3.77 (d, $J = 11.8$ Hz, 1H), 2.74 (s, 3H), 2.07–1.99 (m, 2H), 1.82–1.76 (m, 2H), 1.69–1.58 (m, 2H); ^{13}C NMR (125 MHz, CDCl_3) δ 159.5, 149.0, 148.2, 129.7, 129.3, 125.9, 123.9, 123.1, 118.6, 76.5, 69.6, 34.0, 26.3, 25.8, 24.4. (Spectra data are consistent with those reported in the literature: J. Jin and D. W. C. MacMillan, *Angew. Chem. Int. Ed.*, **2015**, 54, 1565–1569.)

Table 3, entry 7



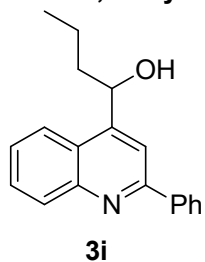
4-(1,4-dioxan-2-yl)-2-methylquinoline (3g). Oil; $R_f = 0.5$ (hexane:EtOAc = 20:1); ^1H NMR (500 MHz, CDCl_3) δ 8.05 (d, $J = 8.5$ Hz, 1H), 7.95 (d, $J = 8.4$ Hz, 1H), 7.68 (t, $J = 7.7$ Hz, 1H), 7.52 (t, $J = 7.7$ Hz, 1H), 7.49 (s, 1H), 5.36 (d, $J = 9.3$ Hz, 1H), 4.12 (d, $J = 11.8$ Hz, 1H), 4.07–4.05 (m, 2H), 3.91–3.88 (m, 1H), 3.84–3.74 (m, 1H), 3.46 (t, $J = 10.5$ Hz, 1H), 2.75 (s, 3H); ^{13}C NMR (125 MHz, CDCl_3) δ 159.2, 147.9, 143.5, 129.7, 129.3, 126.0, 123.6, 122.4, 119.1, 74.2, 72.1, 67.4, 66.7, 25.6. (Spectra data are consistent with those reported in the literature: M. C. Quattrini, S. Fujii, K. Yamada, T. Fukuyama, D. Ravelli, M. Fagnoni and L. Ryu, *Chem. Commun.* **2017**, 53, 2335–2338.)

Table 3, entry 8



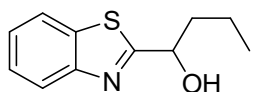
2-phenyl-4-(tetrahydrofuran-2-yl)quinolone (3h). Oil; $R_f = 0.35$ (hexane:EtOAc = 15:1); ^1H NMR (500 MHz, CDCl_3) δ 8.22 (dd, $J = 7.8, 4.7$ Hz, 3H), 8.06 (s, 1H), 7.90 (d, $J = 8.3$ Hz, 1H), 7.72 (t, $J = 7.6$ Hz, 1H), 7.53 (dd, $J = 14.0, 6.8$ Hz, 3H), 7.47 (t, $J = 6.9$ Hz, 1H), 5.66 (t, $J = 7.1$ Hz, 1H), 4.28 (dd, $J = 15.0, 5.7$ Hz, 1H), 4.08 (dd, $J = 15.0, 7.4$ Hz, 1H), 2.68–2.62 (m, 1H), 2.11–1.98 (m, 2H), 1.93–1.86 (m, 1H); ^{13}C NMR (125 MHz, CDCl_3) δ 157.5, 150.0, 148.5, 140.0, 130.7, 129.3, 129.2, 128.8, 127.7, 126.1, 124.6, 123.1, 114.4, 77.1, 69.1, 34.1, 26.1. (Spectra data are consistent with those reported in the literature: C.-Y. Huang, J. Li, W. Liu and C.-J. Li, *Chem. Sci.* **2019**, 10, 5018–5024.)

Table 3, entry 9



1-(2-phenylquinolin-4-yl)butan-1-ol (3i). Oil; $R_f = 0.35$ (hexane:EtOAc = 15:1); ^1H NMR (500 MHz, CDCl_3) δ 8.17 (d, $J = 8.4$ Hz, 1H), 8.00-7.98 (m, 2H), 7.83-7.77 (m, 2H), 7.66 (t, 1H), 7.44-7.42 (m, 4H), 5.31-5.23 (m, 1H), 4.26 (br s, 1H), 1.79-1.74 (m, 2H), 1.55-1.46 (m, 2H), 0.96-0.92 (m, 3H); ^{13}C NMR (125 MHz, CDCl_3) δ 157.2, 151.5, 148.1, 139.4, 130.3, 129.5, 129.3, 128.8, 127.6, 126.1, 124.5, 122.9, 115.2, 69.9, 40.5, 19.3, 13.9; HRMS (ESI-TOF) m/z: [M+H]⁺ Calcd for $\text{C}_{19}\text{H}_{20}\text{NO}$ 278.154; found 278.151.

Table 3, entry 10



3j

1-(benzo[d]thiazol-2-yl)butan-1-ol (3j). Oil; $R_f = 0.35$ (hexane:EtOAc = 5:1); ^1H NMR (500 MHz, CDCl_3) δ 7.98 (d, $J = 8.2$ Hz, 1H), 7.89 (d, $J = 8.0$ Hz, 1H), 7.48 (t, $J = 7.7$ Hz, 1H), 7.38 (t, $J = 7.6$ Hz, 1H), 5.13-5.10 (m, 1H), 3.06 (d, $J = 7.6$ Hz, 1H), 2.05-1.98 (m, 1H), 1.95-1.88 (m, 1H), 1.59-1.52 (m, 2H), 0.99 (t, $J = 10.0$ Hz, 3H); ^{13}C NMR (125 MHz, CDCl_3) δ 176.1, 152.8, 134.9, 126.1, 125.0, 122.9, 121.9, 72.2, 40.2, 18.4, 13.9. (Spectra data are consistent with those reported in the literature: T. He, L. Yu, L. Zhang, L. Wang and M. Wang, *Org. Lett.*, **2011**, *13*, 5016-5019.)

NMR Spectra

^1H NMR and ^{13}C NMR Spectrum of **3a**

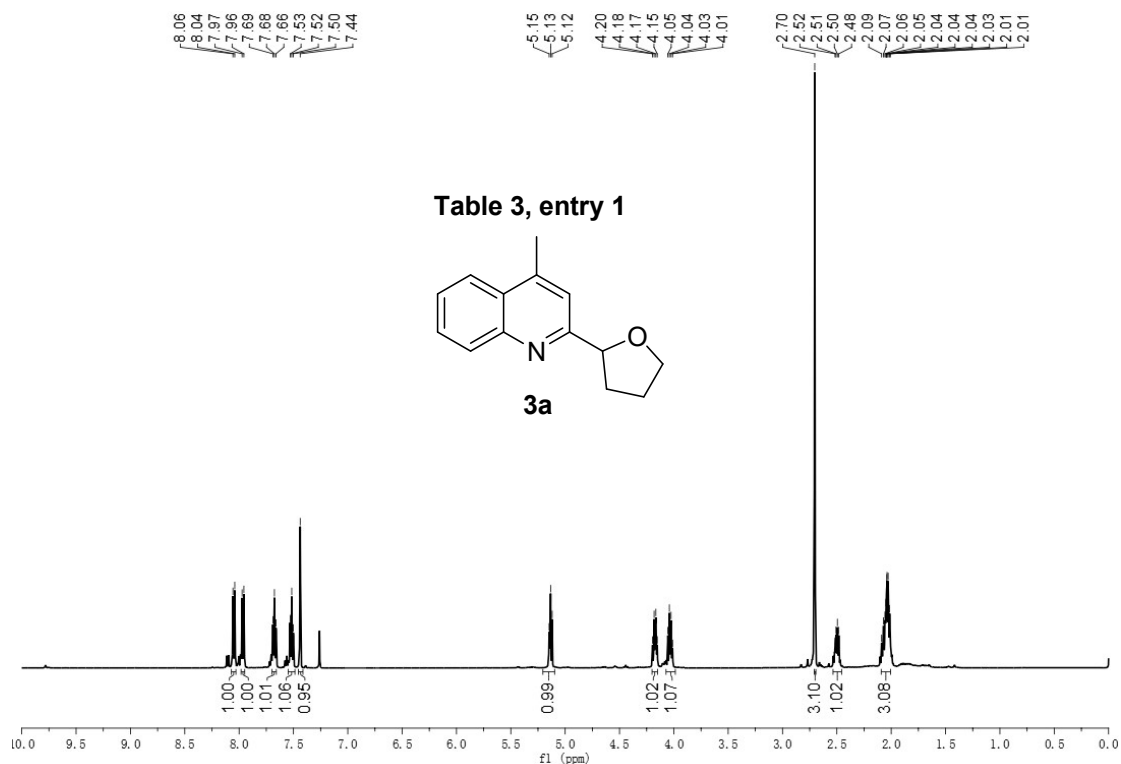
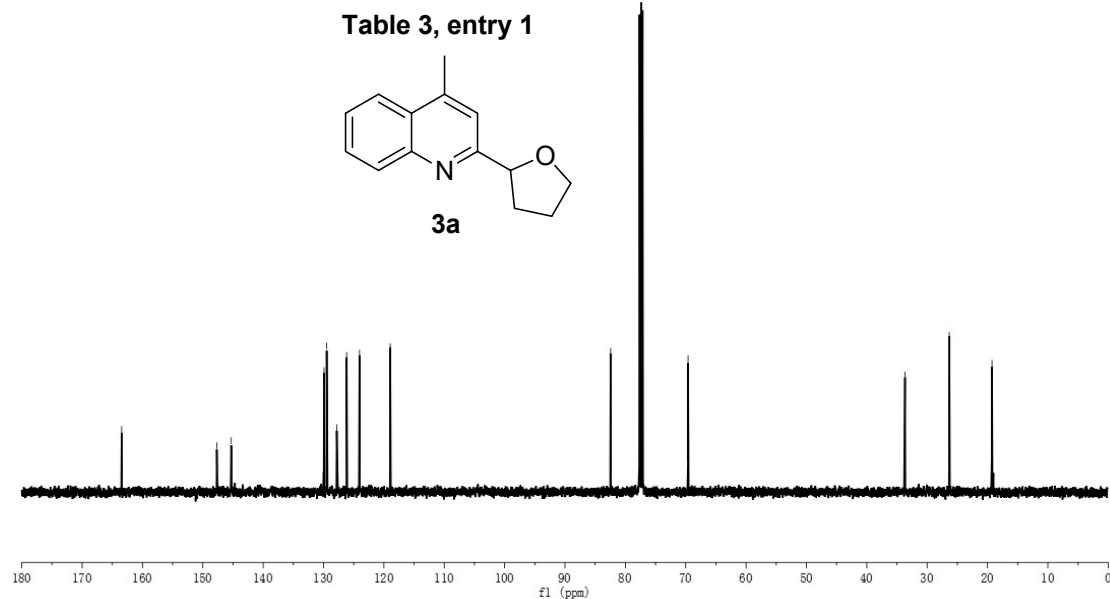


Table 3, entry 1



¹H NMR and ¹³C NMR Spectrum of **3b**

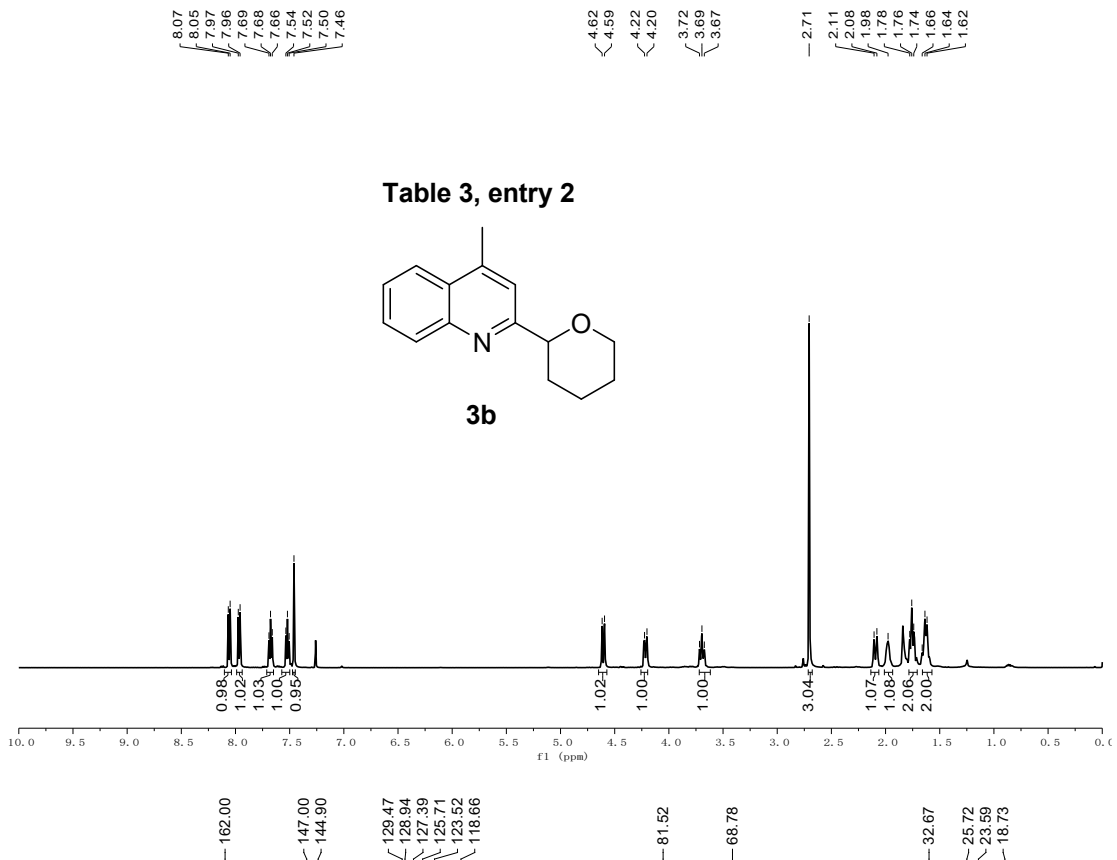
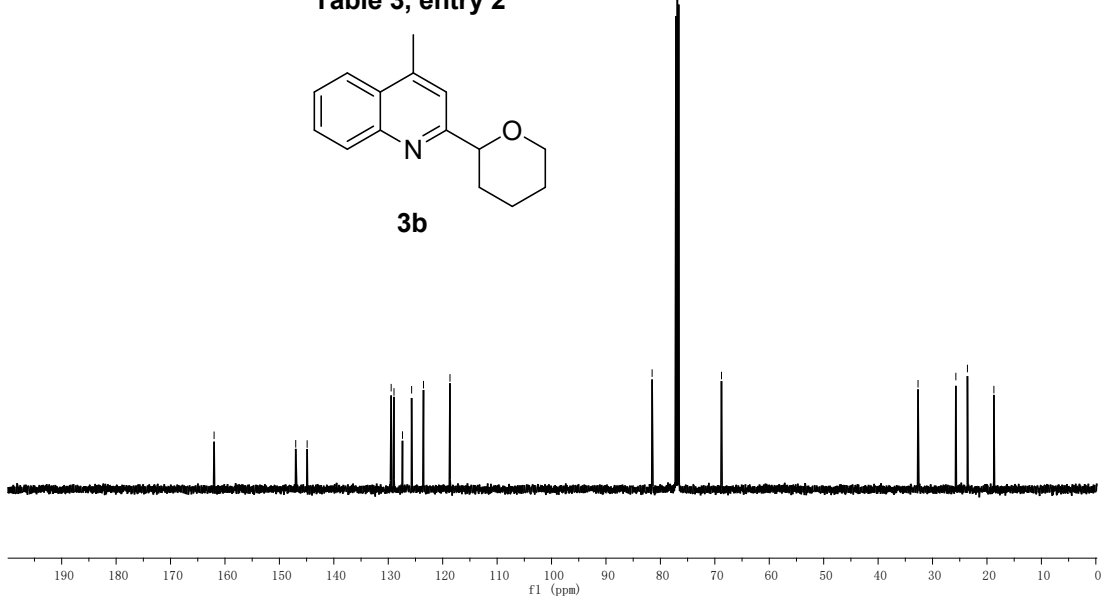


Table 3, entry 2



¹H NMR and ¹³C NMR Spectrum of 3c

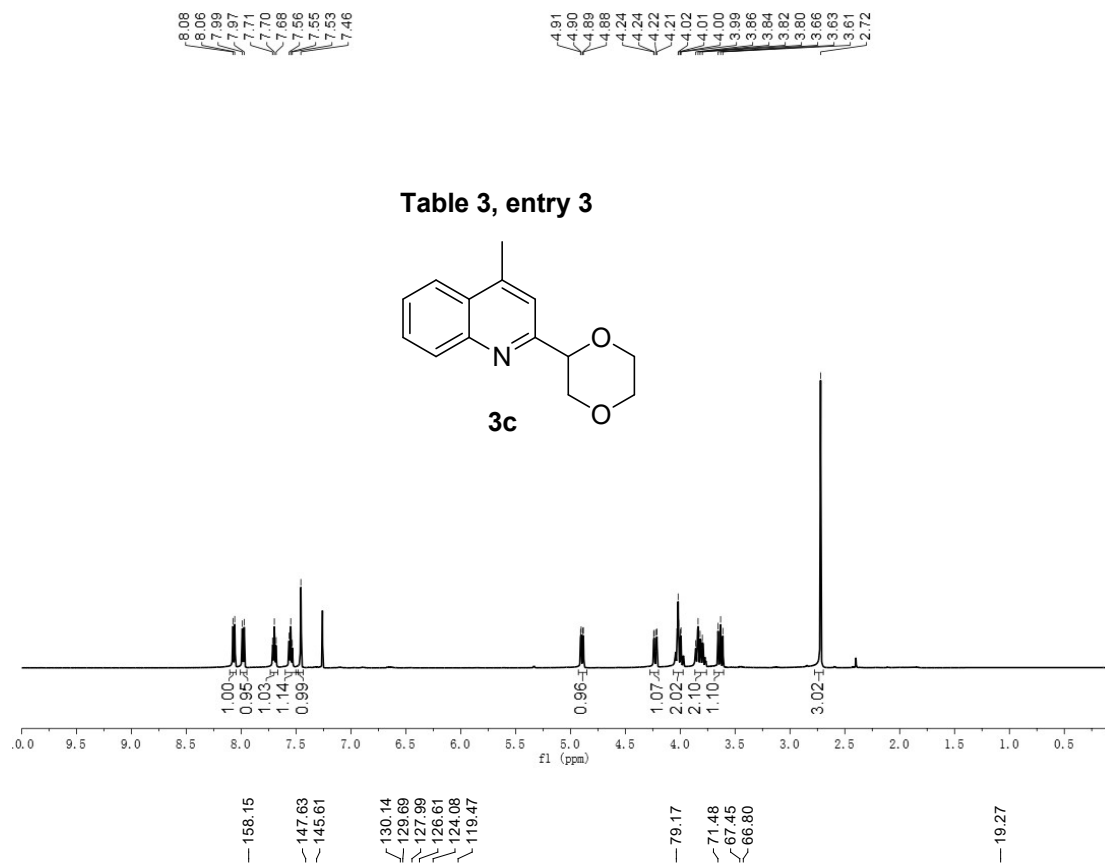
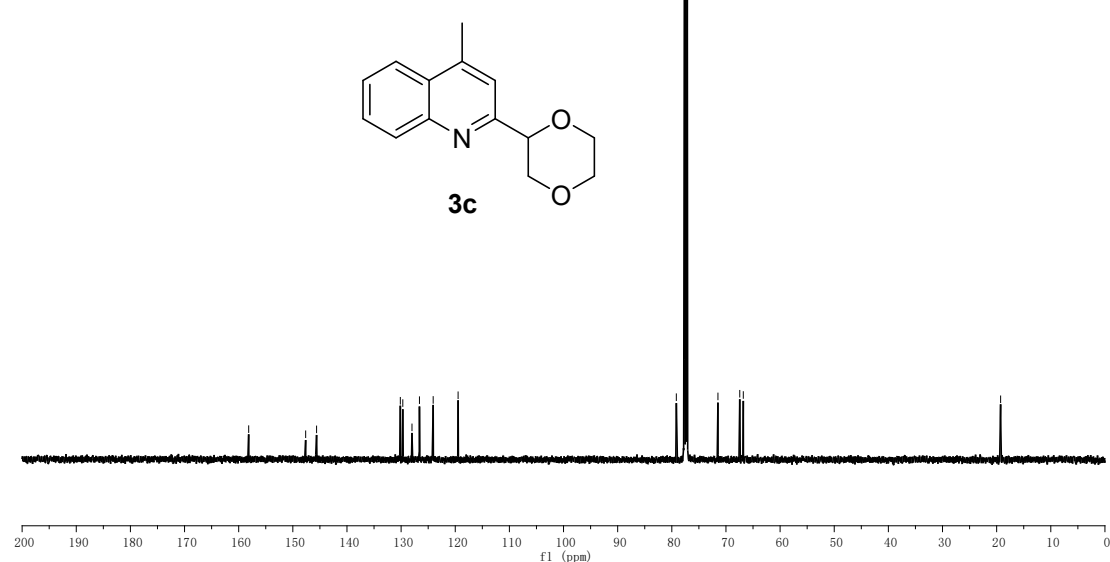


Table 3, entry 3



¹H NMR and ¹³C NMR Spectrum of **3d**

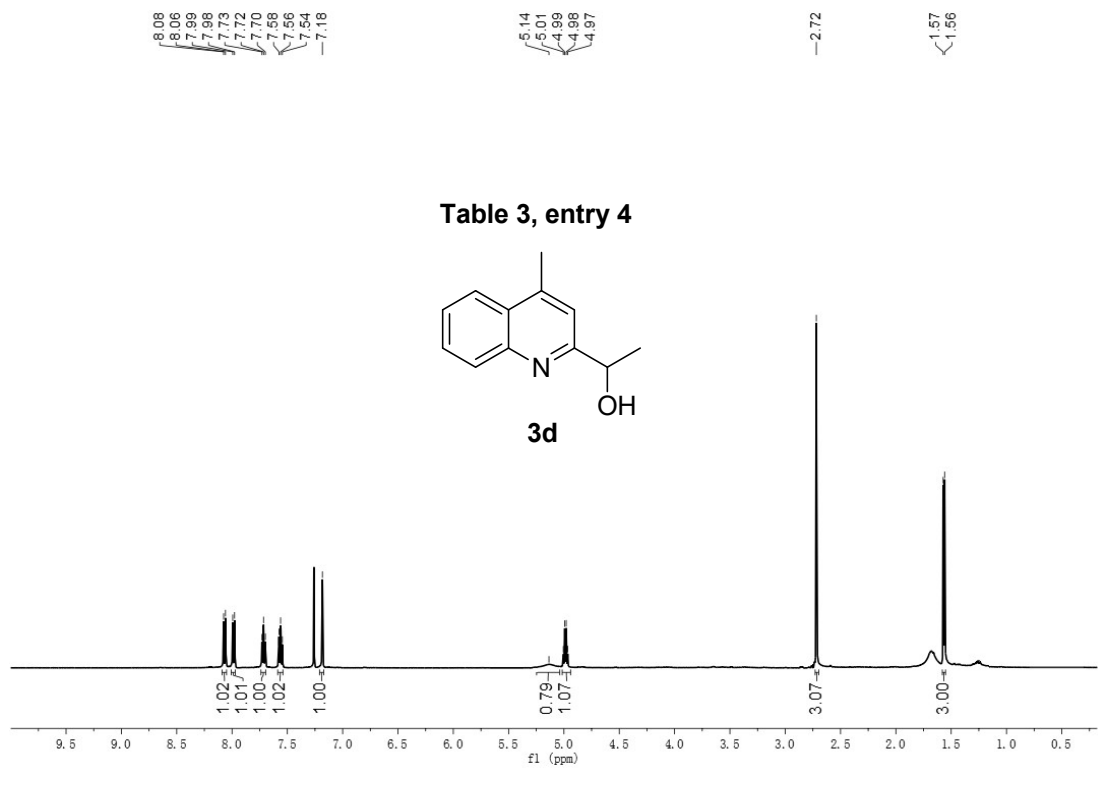
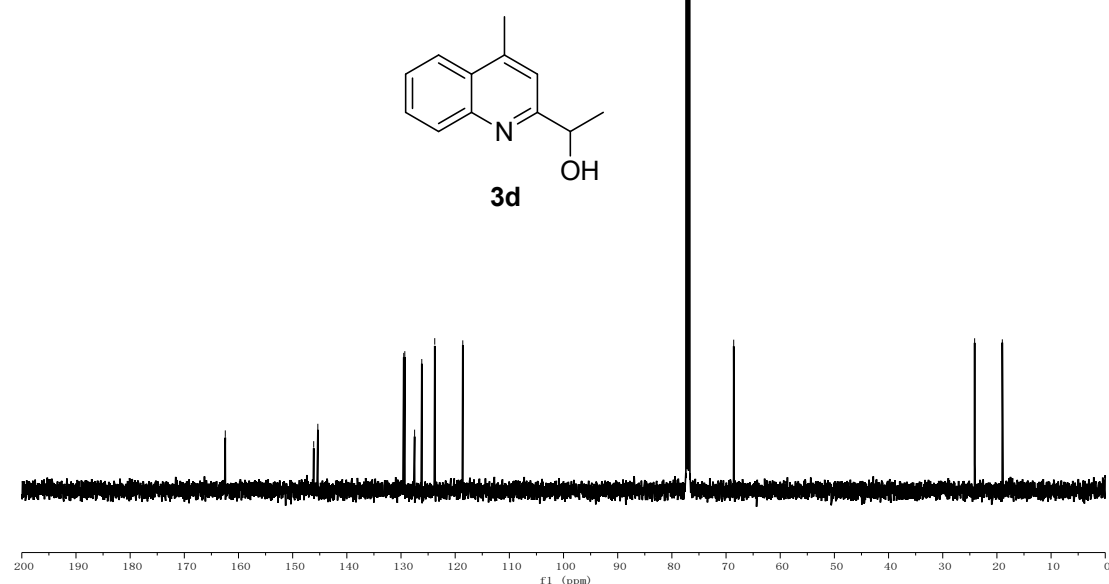
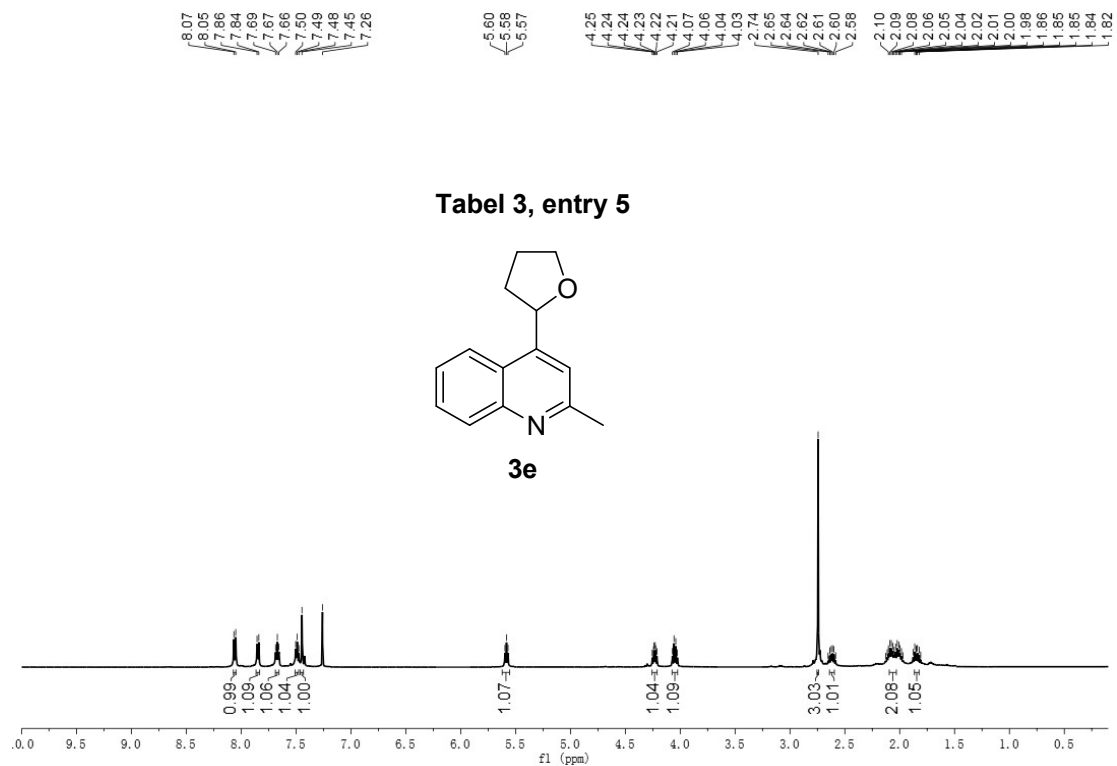


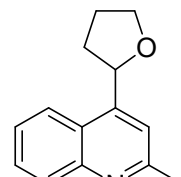
Table 3, entry 4



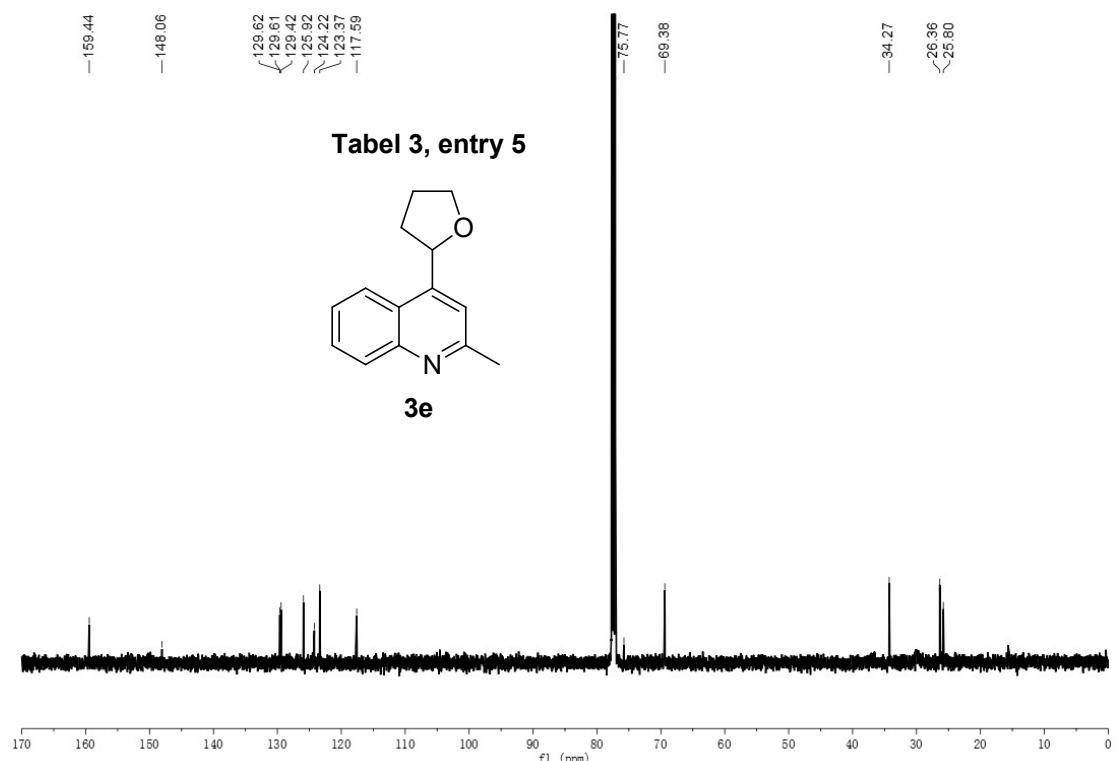
¹H NMR and ¹³C NMR Spectrum of **3e**



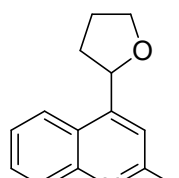
Tabel 3, entry 5



3e



Tabel 3, entry 5



3e

¹H NMR and ¹³C NMR Spectrum of **3f**

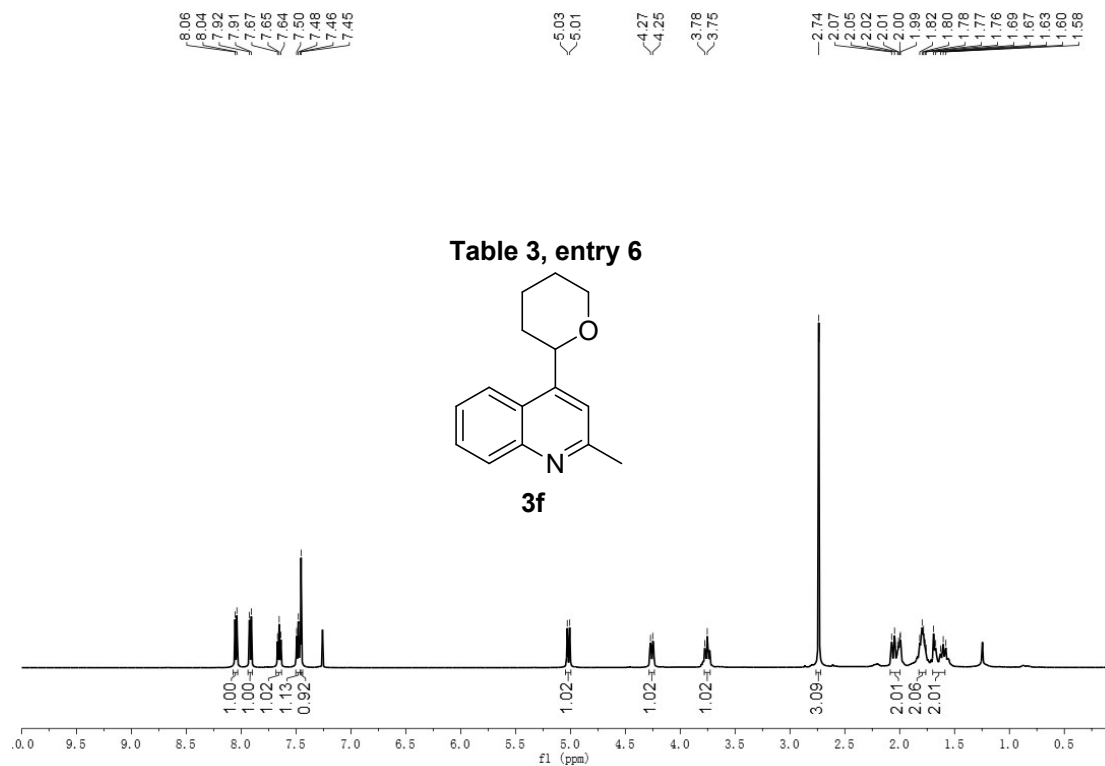
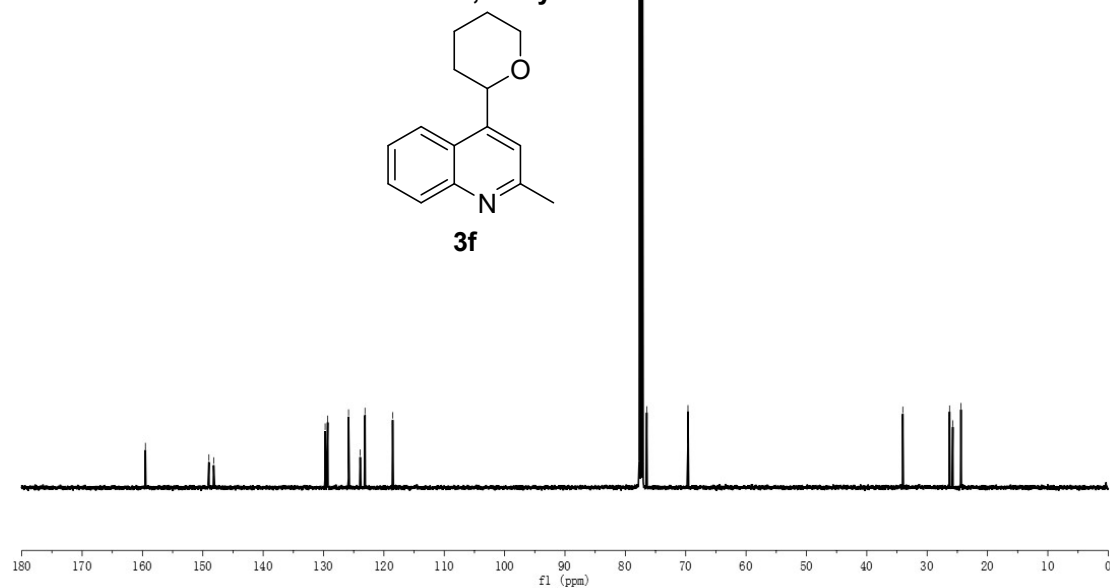


Table 3, entry 6



¹H NMR and ¹³C NMR Spectrum of **3g**

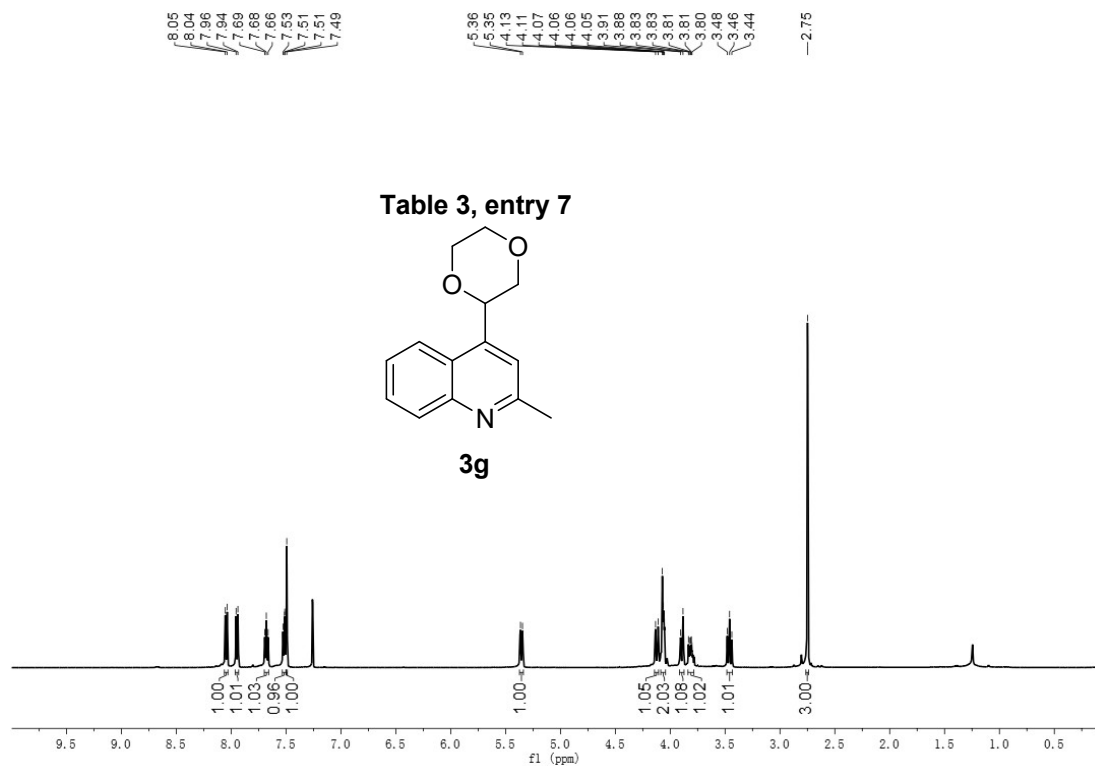
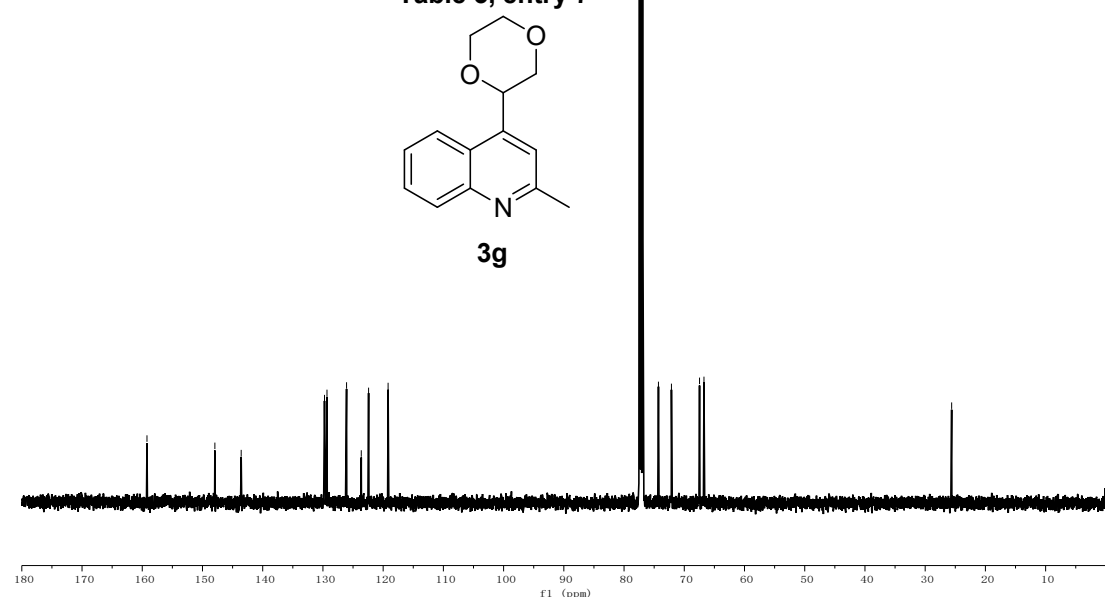


Table 3, entry 7



¹H NMR and ¹³C NMR Spectrum of **3h**

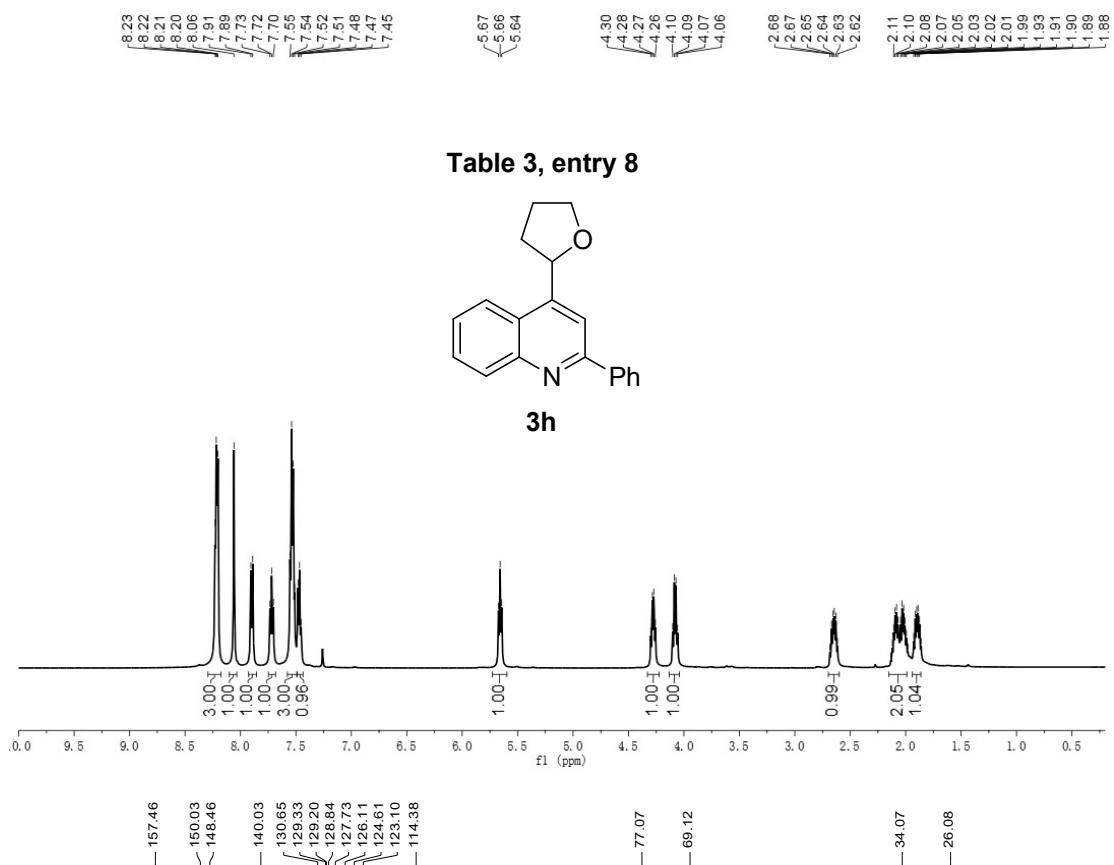
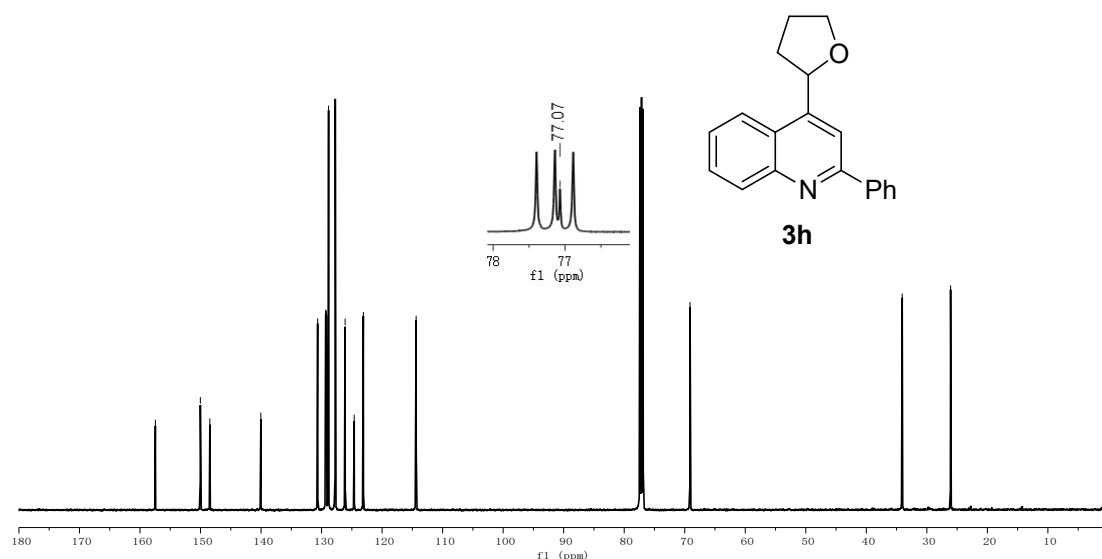


Table 3, entry 8



¹H NMR and ¹³C NMR Spectrum of **3i**

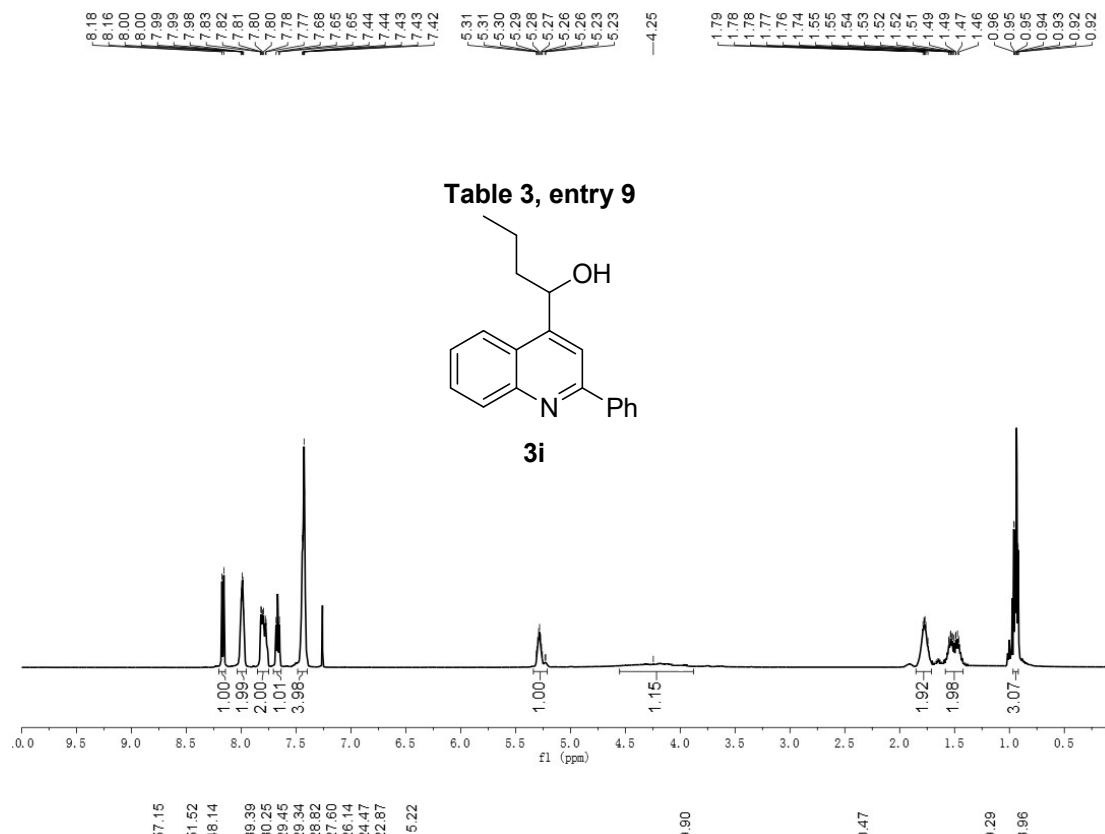
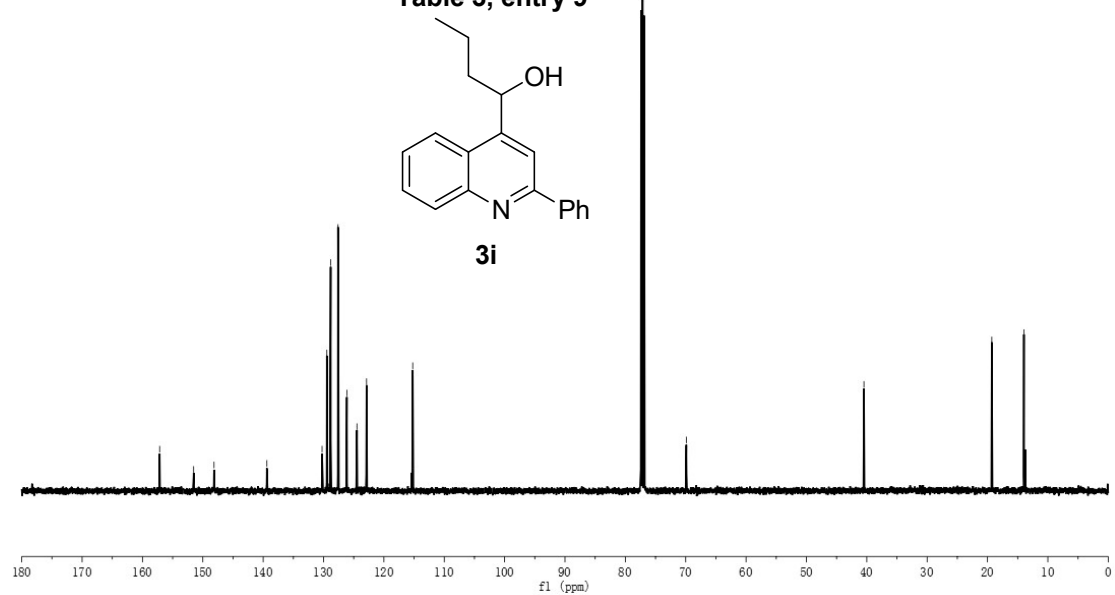
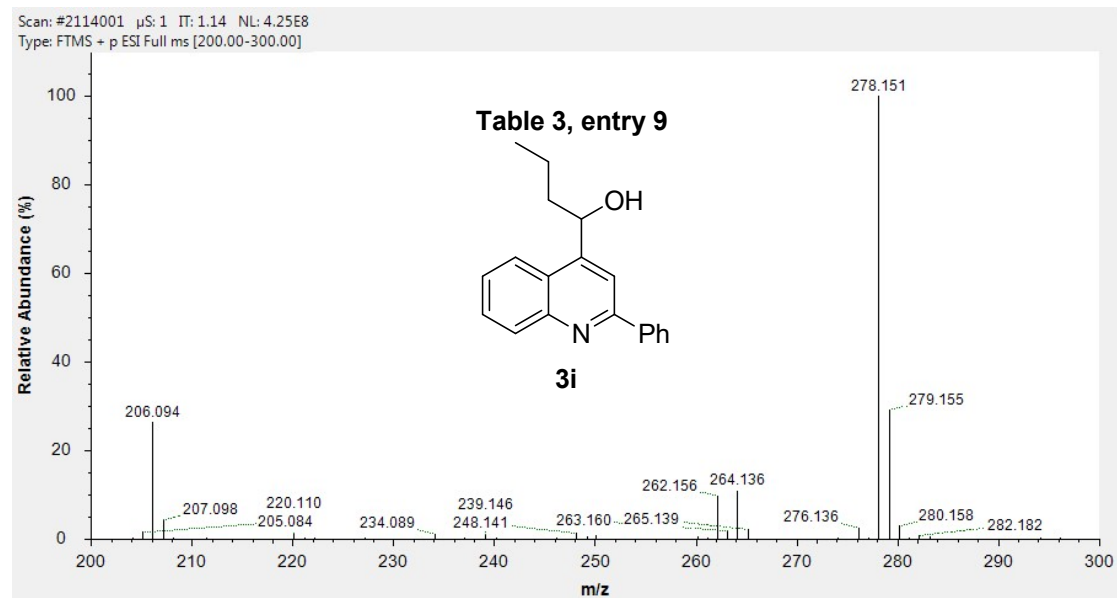


Table 3, entry 9



HRMS of 3i



¹H NMR and ¹³C NMR Spectrum of **3j**

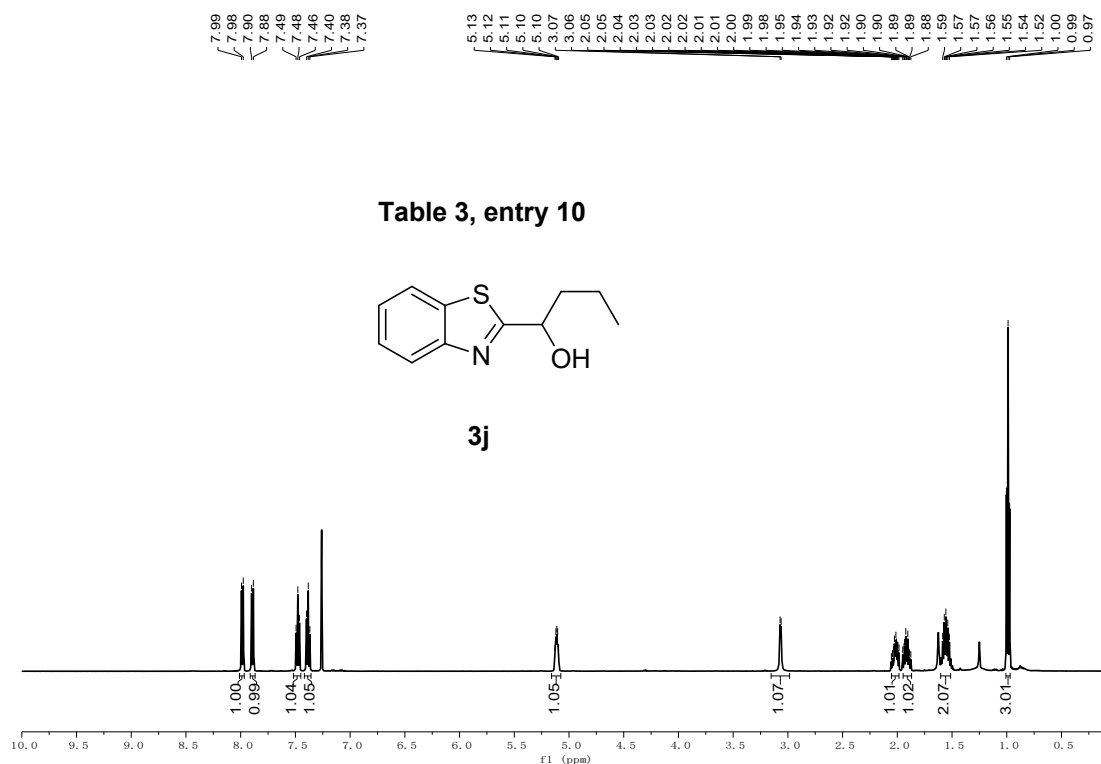


Table 3, entry 10

